Simultaneous Robot/World and Tool/Flange Calibration by Solving Homogeneous Transformation Equations of the Form $AX = YB$

Hanqi Zhuang, Zvi S. Roth, and R. Sudhakar

Abstract—**The paper presents a linear solution that allows a simultaneous computation of the transformations from robot world to robot base and from robot tool to robot flange coordinate frames. The flange frame is defined on the mounting surface of the end-effector. It is assumed that the robot geometry, i.e., the transformation from the robot base frame to the robot flange frame, is known with sufficient accuracy, and that robot end-effector poses are measured. The solution has applications to accurately locating a robot with respect to a reference frame, and a robot sensor with respect to a robot end-effector. The identification problem is cast as solving a system of homogeneous transformation equations of the form $\mathbf{A}_i\mathbf{X} = \mathbf{Y}\mathbf{B}_i, i = 1, 2, \cdots, m$. Quaternion algebra is applied to derive explicit linear solutions for X and Y provided that three robot pose measurements are available. Necessary and sufficient conditions for the uniqueness of the solution are stated. Computationally, the resulting solution algorithm is noniterative, fast and robust.**

I. Introduction

Off-line programming of robots requires accurate knowledge of the robot geometry and the geometric relationships among the robot, its sensors and a reference frame. Fig. 1 illustrates schematically the geometry of a robotic cell. The world coordinate frame is an external reference frame, which is usually defined by the robot calibration measurement setup. The base coordinate frame is normally defined inside the robot structure. Its default location is often provided by the robot manufacturer; however users are allowed to redefine it. The flange coordinate frame is defined on the mounting surface of the robot end-effector. The tool frame is assigned at a convenient location within the end-effector. Formal definitions of homogeneous transformations $\mathbf{A}, \mathbf{B}, \mathbf{X}$ and $\mathbf{Y}$ (shown in Fig. 1) will be given in Section II.

Robot calibration is the process of enhancing the accuracy of a robot manipulator through modification of its control software [1]. This paper addresses a subset of the robot calibration problem; i.e., the calibration problem of robot/world (i.e., the **BASE** transformation) and tool/flange (i.e., the **TOOL** transformation). It is argued that the robot base to flange geometry needs not to be calibrated as often as the other two transformations. In practice, a complete manipulator calibration needs to be done relatively infrequently—for instance after mechanical repair or scheduled maintenance. That is, for a well calibrated manipulator, one may occasionally need to perform partial calibration whenever a tool is changed or whenever the robot world frame is redefined. In the Robotics literature, the most frequently used methods are used on linearized error models. These iterative numerical procedures often require good estimates of initial conditions.

This paper presents a linear solution for the simultaneous identification of both the **BASE** and **TOOL** transformations. This problem is formulated as solving a system of homogeneous transformation equations of the form $\mathbf{A}_i\mathbf{X} = \mathbf{Y}\mathbf{B}_i, i = 1, 2, \cdots, m$, where m is number of pose measurements. The solution approach is motivated by [2], in which the calibration of hand-eye relationship was formulated as solving homogeneous transformation equations of the form $\mathbf{A}_i\mathbf{X} = \mathbf{X}\mathbf{B}_i$. By extending the method presented in [3], quaternion algebra is used to derive a linear solution for $\mathbf{X}$ and $\mathbf{Y}$ from $\mathbf{A}_i\mathbf{X} = \mathbf{Y}\mathbf{B}_i$. The resulting solution algorithm is noniterative, fast and robust.

Manuscript received January 15, 1993; revised July 27, 1993.
The authors are with the Robotics Center and Department of Electrical Engineering, Florida Atlantic University, Boca Raton, FL 33431 USA.
IEEE Log Number 9402090.

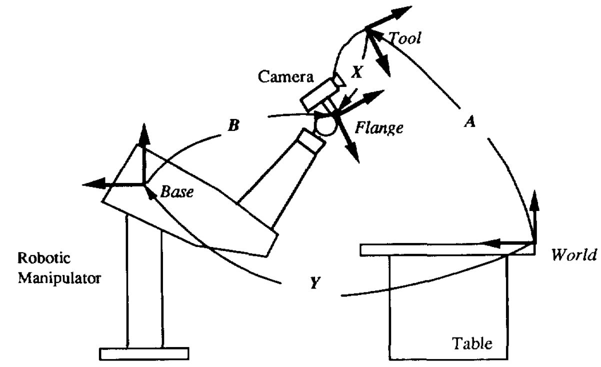

Fig. 1. Geometry of a robotic system.

The paper is organized into the following sections. In Section II, the identification problem of the robot-to-world and tool-to-flange transformations is formulated. The linear solution to the problem is derived in Section III. Performance assessment of the method through simulation is presented in Section IV.

II. Problem Statement

Let $\mathbf{T}_n$ be a 4×4 homogeneous transformation relating the position and orientation of the robot end-effector to the world coordinate frame.

$$\mathbf{T}_n = \mathbf{A}_0\mathbf{A}_1 \cdots \mathbf{A}_{n-1}\mathbf{A}_n \tag{1}$$

Each joint is assumed to be ideal, either revolute or prismatic. $\{\mathbf{i}\}$, a Cartesian coordinate frame $\{x_i, y_i, z_i\}, i = -1, 0, \cdots, n$, is established for each link. The world, base and tool frames are denoted as the -1th, 0th and nth link frames, respectively.

BASE, the transformation from the world to the base frames, is fixed and defined as $\mathbf{BASE} \equiv \mathbf{A}_0$. **FLANGE**, the transformation from the $(n-1)$th to the flange frames, contains the joint variable q_n while **TOOL**, the transformation from the flange to the tool frames, is fixed. Thus $\mathbf{FLANGE} \cdot \mathbf{TOOL} \equiv \mathbf{A}_n$ The robot kinematic model (1) can thus be rewritten as follows:

$$\mathbf{T}_n = \mathbf{BASE} \cdot \mathbf{A}_1 \cdots \mathbf{A}_{n-1} \cdot \mathbf{FLANGE} \cdot \mathbf{TOOL} \tag{2}$$

The nominal values of transformations $\mathbf{A}_1, \cdots, \mathbf{A}_{n-1}$ and **FLANGE** can be obtained from the design specifications of the robot. Their actual values can be estimated using a complete robot calibration process. It is assumed in this paper that these transformations are known with sufficient precision. The **BASE** and **TOOL** transformations are application-dependent, and should be recalibrated more frequently. Since a homogeneous transformation is always invertible, let (Refer to Fig. 1)

$$\mathbf{A} \equiv \mathbf{T}_n \tag{3}$$

$$\mathbf{B} \equiv \mathbf{A}_1 \cdots A_{n-1} \cdot \mathbf{FLANGE} \tag{4}$$

$$\mathbf{X} \equiv \mathbf{TOOL}^{-1} \tag{5}$$

$$\mathbf{Y} \equiv \mathbf{BASE} \tag{6}$$

Then by (2),

$$\mathbf{AX} = \mathbf{YB} \tag{7}$$

1042-296X/94$04.00 © 1994 IEEE

The homogeneous transformation $\mathbf{A}$ is known from end-effector pose measurements, $\mathbf{B}$ is computed using the calibrated manipulator internal-link forward kinematics, $\mathbf{X}$ is the inverse unknown **TOOL** transformation, and $\mathbf{Y}$ is the unknown **BASE** transformation.

The problem is now reduced to that of solving a system of matrix equations of the type (7). That is, $\mathbf{X}$ and $\mathbf{Y}$ are to be determined uniquely from (7), given $\mathbf{A}_i$ and $\mathbf{B}_i$, which are obtained from different measurement configurations.

III. A Linear Solution of the Equations $\mathbf{AX} = \mathbf{YB}$

Let R_A, R_X, R_Y and R_B be the respective 3×3 rotation matrices of A, X, Y and B, and let $\mathbf{p}_A$, $\mathbf{p}_X$, $\mathbf{p}_Y$ and $\mathbf{p}_B$ be the respective 3×1 translational vectors. Equation (7) can then be decomposed into a rotation equation (8) and a position equation (9),

$$R_A R_X = R_Y R_B \tag{8}$$

$$R_A \mathbf{p}_X + \mathbf{p}_A = R_Y \mathbf{p}_B + \mathbf{p}_Y. \tag{9}$$

Equation (9) is a linear equation in p_X and p_Y if R_Y is known. Upon obtaining R_X and R_Y, $\mathbf{p}_X$ and $\mathbf{p}_Y$ may be solved linearly from a set of equations of the type (9). We thus first focus on the linear solution of the rotation equation (8).

A. Solution of R_X and R_Y

Readers are referred to [4], [5] for background materials on quaternions.

Let $\mathbf{a} \equiv (a_0, a), \mathbf{b} \equiv (b_0, b), \mathbf{x} \equiv (x_0, x)$ and $\mathbf{y} \equiv (y_0, y)$ be unit quaternions that correspond to the rotation matrices R_A, R_B, R_X and R_Y. Note that a_0 and a are the scalar and 3×1 vector parts of $\mathbf{a}$. Similar for other notations. Let $\mathbf{u}_j$ and $\mathbf{b}_j$ be the jth column vector of the identity matrix and the $\mathbf{B}$ matrix, respectively. The vectors correspond to the respective pure quaternions $\mathbf{u}_j$ and $\mathbf{b}_j$. Let $\circ$ denote a quaternion product. Finally, for any rotation matrix R, let $R = \mathrm{Rot}(\mathbf{k}, \theta)$, where $\mathbf{k}$ and θ are respectively the rotation axis and rotation angle.

Lemma 3.1: The rotation equation $R_A R_X = R_Y R_B$ is equivalent to the following quaternions equation

$$\mathbf{a} \circ \mathbf{x} = \mathbf{y} \circ \mathbf{b} \tag{10}$$

This fact is a straightforward extension of some of the results given in [3]–[5].

Let $\mathrm{v} \equiv [v_1 \quad v_2 \quad v_3]^t$, where the superscript t denotes matrix transpose. For convenience of notation, define the skew-symmetric matrix function $\Omega(\mathrm{v})$ as

$$\Omega(\mathbf{v}) \equiv \begin{bmatrix} 0 & -v_3 & v_2 \\ v_3 & 0 & -v_1 \\ -v_2 & v_1 & 0 \end{bmatrix} \tag{11}$$

Also define a 6×1 vector $\mathbf{w}$ and a 3×1 vector $\mathbf{c}$ as follows

$$\mathbf{w} \equiv [x^t/y_0, y^t/y_0]^t \tag{12}$$

$$c \equiv b - (b_0/a_0)\mathbf{a} \tag{13}$$

and a 3×6 matrix G as

$$G \equiv [a_0 I + \Omega(a) + aa^t/a_0, -b_0 I + \Omega(b) - ab^t/a^0] \tag{14}$$

Lemma 3.2: If $\theta_A \neq \pi$ and $\theta_Y \neq \pi$, then $R_A R_X = R_Y R_B$ is equivalent to the vector equation

$$G\mathbf{w} = c \tag{15}$$

Proof: Expanding (10) using quaternion products yields

$$\begin{aligned}(a_0 x_0 - a \cdot \mathbf{x}, a_0 \mathbf{x} + x_0 b + a \times \mathbf{x}) \\ = (b_0 y_0 - b \cdot \mathbf{y}, b_0 \mathbf{y} + y_0 b - b \times \mathbf{y})\end{aligned} \tag{16}$$

where $\cdot$ and $\times$ denote vector and dot products, respectively. If $\theta_A \neq \pi$, then $a_0 \neq 0$. x_0 can be solved from the scalar part of (16),

$$x_0 = (a/a_0) \cdot \mathbf{x} + (b_0/a_0)y - (b/a_0) \cdot \mathbf{y} \tag{17}$$

Substituting (17) into the vector part of (16) yields

$$\begin{aligned}[(b_0/a_0)a - b]y_0 + a_0 x + a(a/a_0) \cdot \mathbf{x} - a(b/a_0) \cdot y - b_0 y \\ + a \times \mathbf{x} + b \times y = 0\end{aligned} \tag{18}$$

If $\theta_Y \neq \pi$, then $y_0 \neq 0$. Dividing both sides of (18) by y_0, yields

$$\begin{aligned}(a_0 \mathbf{I} + \Omega(a) + aa^t/a_0)\mathbf{x}/y_0 + (-b_0 \mathbf{I} + \Omega(b) - ab^t/a_0)y/y_0 \\ = b - (b_0/a_0)a\end{aligned} \tag{19}$$

where use has been made of the relationship $\mathbf{v} \times \mathbf{x} = \Omega(\mathbf{v})\mathbf{x}$ for $\mathbf{v} = a$ or b. Finally, by the definitions of G, $\mathbf{w}$ and $\mathbf{c}$, (15) is obtained. Q.E.D.

Let us examine under what conditions $\theta_A = \pi$ occurs. Let

$$R_A \equiv \begin{bmatrix} n_x & o_x & a_x \\ n_y & o_y & a_y \\ n_z & o_z & a_z \end{bmatrix}$$

According to [6],

$$2\cos\theta_A = n_x + o_y + a_z - 1 \tag{20a}$$

and

$$4\sin^2\theta_A = (o_z - a_y)^2 + (a_x - n_z)^2 + (n_y - o_x)^2 \tag{20b}$$

Therefore, $\theta_A = \pi$ is equivalent to the following set of conditions,

$$n_x + o_y + a_z = -1 \tag{21a}$$

$$o_z - a_y = 0 \tag{21b}$$

$$a_x - n_z = 0 \tag{21c}$$

$$n_y - o_x = 0 \tag{21d}$$

These conditions can be checked for each measurement configuration, and if satisfied this pose shall be avoided.

A similar analysis can be done to identify the conditions under which $\theta_Y = \pi$ occurs. Care has to be taken when placing either the base frame or the world frame.

Example: A rotation R_A that satisfies the conditions given in (21) is shown below:

$$R_A \equiv \begin{bmatrix} -1 & 0 & 0 \\ 0 & 0 & 1 \\ 0 & 1 & 0 \end{bmatrix}$$

In this example, the tool frame can be obtained by rotating the world frame 180°about the axis $[0, \quad 0.707, \quad 0.707]^T$.

Equation (15) consists of three scalar equations with six unknowns. A unique solution of $\mathbf{w}$ therefore requires multiple measurements. Let

$$\mathbf{Gw} = \mathbf{C} \tag{22}$$

where $\mathbf{G}$((3m) $\times$ 6 matrix) and $\mathbf{C}$ ((3m) $\times$ 1 vector) are defined as

$$\mathbf{G} \equiv \begin{bmatrix} G_1 \\ G_2 \\ \vdots \\ G_m \end{bmatrix} \tag{23a}$$

$$\mathbf{C} \equiv \begin{bmatrix} \mathbf{c}_1 \\ \mathbf{c}_2 \\ \vdots \\ \mathbf{c}_m \end{bmatrix} \tag{23b}$$

In (23), G_i and $\mathbf{c}_i$ have, respectively, the same structure as G and c in (14) and (13). The Singular Value Decomposition algorithm can be applied to solve for $\mathbf{w}$. After $\mathbf{w} \equiv [w_1 \quad w_2 \quad w_3 \quad w_4 \quad w_5 \quad w_6]^t$ is obtained, $\mathbf{x}$ and $\mathbf{y}$ can be determined from (12) using the constraints $\mathbf{yy}^* = \mathbf{xx}^* = 1$ and (17). More specifically,

$$y_0 = \pm\{1 + w_4^2 + w_5^2 + w_6^2\}^{-1/2} \tag{24a}$$

$$\mathbf{y} = y_0[w_4 \quad w_5 \quad w_6]^t \tag{24b}$$

$$\mathbf{x} = y_0[w_1 \quad w_2 \quad w_3]^t \tag{24c}$$

$$x_0 = \pm\{1 - x_1^2 - x_2^2 - x_3^2\}^{-1/2}. \tag{24d}$$

Since $\pm\mathbf{q}$, where $\mathbf{q}$ is an arbitrary quaternion, correspond to the same rotation matrix R_q, one needs only to determine the sign of x_0 by using (17).

Before proving that at least three measurements are required to obtain a unique solution, the following simplifications are made:

Assume that there are three rotation equations,

$$R_{Ai}R_X = R_Y R_{Bi} \qquad i = 1, 2, 3 \tag{25}$$

Let $R'_X \equiv R_{A1}R_X$, and $R'_Y \equiv R_Y R_{B1}$. Then (26) given next is equivalent to (25) since once R'_X and R'_Y are obtained, R_X and R_Y can be determined uniquely.

$$R'_X = R'_Y \tag{26a}$$

$$R'_{A_i}R'_X = R'_Y R'_{B_i} \qquad i = 2, 3 \tag{26b}$$

where $R'_{Ai} \equiv R_{Ai}R^t_{A1}$, and $R'_{Bi} \equiv R^t_{B1}R_{Bi}$. By (26a), R'_{A2} and R'_{B2} in (26b) must have the same rotation angle [4, Lemma 4]. Define

$$R^t_{A_i}R_{A1} = \mathrm{Rot}(k'_{Ai}, \beta_i) \qquad i = 2, 3 \tag{27a}$$

$$R^t_{B1}R_{Bi} = \mathrm{Rot}(k'_{Bi}, \beta_i) \qquad i = 2, 3 \tag{27b}$$

β_i, termed the ith *relative rotation angle*, plays a role in determining the uniqueness of the solution for both the rotation matrices and the position vectors.

Theorem 3.1: A necessary condition for unique identification of R_X and R_Y from (22) is that $m \geq 3$, where m is the number of pose measurements.

Proof: Let $m = 2$. By (26), the 6×6 matrix $\mathbf{G}$ in (23a) is reduced to

$$\mathbf{G} \equiv \begin{bmatrix} I_{3\times3} & -I_{3\times3} \\ G_{A2} & G_{B2} \end{bmatrix} \tag{28}$$

where $[G_{A2}G_{B2}] \equiv G_2$. By elementary matrix transformations, $\mathbf{G}$ in (28) can be reduced to

$$\mathbf{G} \equiv \begin{bmatrix} I_{3\times3} & 0_{3\times3} \\ 0_{3\times3} & G_{A2+G_{B2}} \end{bmatrix} \tag{29}$$

A necessary and sufficient condition for (20) to have a unique solution is that $\mathrm{Rank}(\mathbf{G}) = 6$, or equivalently, $\mathrm{Rank}(G_{A2} + G_{B2}) = 3$. By using the software package **MACSYMA** [7], $G_{A2} + G_{B2}$ can be triangularized and simplified. The resulting three diagonal elements after simplification are $\{-k_{B2,1}(k_{B2,1} - k_{A2,1})\sin^2(\beta_2), -(k_{B2,3} + k_{A2,3})((k_{A2,1}k_{B2,2} - k_{A2,2}k_{B2,1})\sin(\beta_2) - (k_{A2,3} + k_{B2,3})\cos(\beta_2), 0\}$, where $[k_{A2,1}\, k_{A2,2}\, k_{A2,3}]^t \equiv \mathbf{k}_{A2'}$ and $[k_{b2,1}\, k_{b2,2}\, k_{B2,3}]^t \equiv \mathbf{k}_{B2'}$. Since the third diagonal element of the reduced matrix is zero, $\mathrm{Rank}(G_{A2} + G_{B2}) < 3$. Consequently for a unique solution of $\mathbf{w}$, $m > 2$. Q.E.D.

Three pose measurements are not always sufficient for obtaining a unique solution of (22), as can be seen in the following theorem.

Theorem 3.2: Let $m = 3$. If the axes of rotation for $R_{A2'}$ and $R_{A3'}$ are neither parallel nor antiparallel one to another and the relative rotation angles β_2 and β_3 are both neither zero nor π, then there exists a unique solution of R_X and R_Y.

Proof: Substituting (26a) into (26b) yields

$$R'_{A_i}R'_X = R'_X R'_{Bi} \qquad i = 2, 3$$

The problem is now reduced to that of a robot wrist-mounted sensor calibration, which has been solved in [2], [8]. After R'_X is obtained, R_X and R_Y can be computed from $R'_X \equiv R_{A1}R_X$ and $R'_X \equiv R_Y R_{B1}$, respectively. Q.E.D.

As seen in the above theorem, three pose measurements yield only two relative measurement equations.

Theorem 3.2 also implies that the orientation of the robot end-effector has to be changed from one measurement configuration to another to guarantee the existence of solution for the unknown rotation matrices. The conditions that the relative angle $\beta_i = \pi$ occurs are similar to those given in (21), with the modification that the rotation R_A is replaced by the relative rotation $R^t_{A_i}R_{A1}$.

B. Solution of $\mathbf{p}_Y$ and $\mathbf{p}_B$

Following the solution of R_x and R_y, $\mathbf{p}_X$ and $\mathbf{p}_Y$ become readily computable. Equation (9) can be rewritten as

$$\mathbf{F}\begin{bmatrix} \mathbf{p}_X \\ \mathbf{p}_Y \end{bmatrix} = \mathbf{d} \tag{30}$$

where F(a 3×6 matrix) and $\mathbf{d}$(a 3×1 vector) are defined as

$$F \equiv [R_A, -I_{3\times3}] \tag{31a}$$

$$\mathbf{d} \equiv R_Y\mathbf{p}_B - \mathbf{p}_A \tag{31b}$$

If more than one measurement are provided, let

$$\mathbf{F}\begin{bmatrix} \mathbf{p}_X \\ \mathbf{p}_Y \end{bmatrix} = \mathbf{D} \tag{32}$$

where $\mathbf{F}$ (a (3m) $\times$ 6 matrix) and $\mathbf{d}$ (a (3m) $\times$ 1 vector) are defined similarly to the definitions given in (23). Again the Singular Value Decomposition algorithm can be applied to solve for $\mathbf{p}_Y$ and $\mathbf{p}_B$.

It will be shown that at least three measurements have to be used to have a unique solution of (32). Recall that R_{Ai} is the ith measurement of R_A, and

$$R^t_{A_i}R_{A1} = \mathrm{Rot}(k'_{Ai}, \beta_i) \qquad i = 2, 3$$

$\mathrm{Rot}(k'_{Ai}, \beta_i)$ can be decomposed into [2]

$$\mathrm{Rot}(k'_{A_i}, \beta_i) = E_i H_i E_i^{-1} \qquad i = 2, 3 \tag{33}$$

where

$$\mathbf{H}_i \equiv \begin{bmatrix} 1 & 0 & 0 \\ 0 & e^{j\beta_i} & 0 \\ 0 & 0 & e^{-j\beta_i} \end{bmatrix} \tag{34}$$

and E_i is an orthogonal matrix whose columns consist of the eigenvectors of $R(k'_{Ai}, \beta_i)$. Furthermore,

$$E_i^{-1} = E_i^t \qquad i = 2, 3 \tag{35}$$

after the eigenvectors are normalized.

Theorem 3.3: Given R_X and R_Y, the necessary and sufficient conditions for a unique solution of $\mathbf{p}_X$ and $\mathbf{p}_Y$ from (32) is that

(i) $m = 3$; and
(ii) $R_{Ai} \neq R_{Aj}$ for $i, j \in \{1, 2, 3\}$ and $i \neq j$.

Proof: We note that since all rotations R_{Ai} must be different from one another, $\beta_i \neq 0$ and $\beta_i \neq \beta_j$ for $i, j \in \{2, 3\}$ and $i \neq j$. This is because β_i is a relative rotation angle. If β_i equals zero, then the ith measurement is identical to the first measurement, and the number of measurements is reduced. Similarly for the case that $\beta_i = \beta_j$. Let $m = 3$,

$$\mathbf{F} \equiv \begin{bmatrix} \mathbf{R}_{A1} & -I_{3\times3} \\ \mathbf{R}_{A2} & -I_{3\times3} \\ \mathbf{R}_{A3} & -I_{3\times3} \end{bmatrix} \tag{36}$$

If rank $(\mathbf{F}) = 6$, a unique solution can be obtained since (31) is consistent in the absence of measurement noise. Following a sequence of elementary transformations, $\mathbf{F}$ can be written as

$$\mathbf{F} = \mathbf{P}\mathbf{F}_1\mathbf{Q} \tag{37}$$

where $\mathbf{P}$ is a 9×9 nonsingular matrix and $\mathbf{Q}$ is a 6×6 nonsingular matrix, and

$$\mathbf{F}_1 \equiv \begin{bmatrix} 0_{3\times3} & -I_{3\times3} \\ (\mathrm{Rot}(\mathbf{k}_{A2'}, \beta_2) - I)R_{A1} & 0_{3\times3} \\ (\mathrm{Rot}(\mathbf{k}_{A3'}, \beta_3) - I)R_{A1} & 0_{3\times3} \end{bmatrix} \tag{38}$$

where $R(\mathbf{k}_{Ai'}, \beta_i)$ is defined in (33). Since both $\mathbf{P}$ and $\mathbf{Q}$ are full rank, the solution condition is reduced to rank$(\mathbf{F}_1) = 6$. By (33), $\mathbf{F}_1$ can be further decomposed as follows

$$\begin{aligned} \mathbf{F}_1 = & \begin{bmatrix} I_{3\times3} & 0_{3\times3} & 0_{3\times3} \\ 0_{3\times3} & E_2 & 0_{3\times3} \\ 0_{3\times3} & 0_{3\times3} & E_3 \end{bmatrix} \\ & \begin{bmatrix} 0_{3\times3} & -I_{3\times3} \\ (H_2 - I)E_2^t & 0_{3\times3} \\ (H_3 - I)E_3^t & 0_{3\times3} \end{bmatrix} \\ & \begin{bmatrix} I_{3\times3} & O_{3\times3} \\ O_{3\times3} & R_{A1} \end{bmatrix} \\ \equiv & \mathbf{F}_{11}\mathbf{F}_{12}\mathbf{F}_{13} \end{aligned} \tag{39}$$

Rank$(\mathbf{F}_1)$ = Rank$(\mathbf{F}_{12})$ since $\mathbf{F}_{11}$ and $\mathbf{F}_{13}$ are full rank. Let $E_i \equiv [\mathbf{e}_{i1} \quad \mathbf{e}_{i2} \quad \mathbf{e}_{i3}]$. Then

$$(I - H_i)E_i^t = \begin{bmatrix} O_{1\times3} \\ (1 - e^{j\beta_i})e_{i2}^t \\ (1 - e^{-j\beta_i})e_{i3}^t \end{bmatrix} \tag{40}$$

for $i = 2, 3$. $\mathbf{e}_{32}$ and $\mathbf{e}_{33}$ are not simultaneous linear combinations of $\mathbf{e}_{22}$ and $\mathbf{e}_{23}$ if $\beta_2 \neq \beta_3$ since $\mathbf{e}_{32}$ and $\mathbf{e}_{33}$ do not simultaneously lie on the plane spanned by $\mathbf{e}_{22}$ and $\mathbf{e}_{23}$. The coefficients $1 - e^{j\beta_i} \neq 0$ and $1 - e^{-j\beta_i} \neq 0$ for $i = 2, 3$ if $\beta_2 \neq 0$ and $\beta_3 \neq 0$. Thus there are three independent vectors among $(1 - e^{j\beta_2})\mathbf{e}_{22}$, $(1 - e^{-j\beta_2})\mathbf{e}_{23}$, $(1 - e^{j\beta_3})\mathbf{e}_{32}$, and $(1 - e^{-j\beta_3})\mathbf{e}_{33}$ if $\beta_2 \neq 0$, $\beta_3 \neq 0$, and $\beta_i \neq \beta_j$. Consequently Rank$(\mathbf{F}_{12}) = 6$, and a unique solution can be determined by solving (32).

The proof of the "necessary" part is trivial. If $m = 2$, then Rank$(\mathbf{F}_{12}) \leq 5$ since Rank$((I - H_2)E_2^t) \leq 2$ by checking (40). In this case, $\mathbf{F}$ is singular therefore there is no unique solution for $\mathbf{p}_X$ and $\mathbf{p}_Y$. By the argument given in the proof of the sufficient condition, $\mathbf{F}$ is also singular if $R_{Ai} = R_{Aj}$ for any $i, j \in \{2, 3\}$ and $i \neq j$. Q.E.D.

In summary, to obtain the homogeneous transformations $\mathbf{X}$ and $\mathbf{Y}$ from homogeneous transformation equations of the form $\mathbf{AX} = \mathbf{YB}$, three or more different robot pose measurements are required. The rotation angles θ_{Ai} must not be equal to π when solving for rotation matrices R_X and R_Y from (22). Furthermore, while changing the orientation of the robot end-effector, one should avoid moving the robot end-effector to certain poses specified by (21). The overall solution procedure is as follows:

1) Equation (22) is used to compute the vector $\mathbf{w}$ using measurement data.
2) Equation (24) is then used to compute $\mathbf{x}$ and $\mathbf{y}$ from $\mathbf{w}$.
3) R_X and R_y are recovered from from $\mathbf{x}$ and $\mathbf{y}$ [4], [5].
4) Equation (32) is used to compute $\mathbf{p}_X$ and $\mathbf{p}_Y$ using the measurement data as well as the computed R_X and R_y.

TABLE I
THE NOMINAL D–H PARAMETERS OF THE PUMA 560

i	θ_i (deg)	d_i (mm)	α_i (deg)	a_i (mm)
1	90.0	0	-90	0
2	0.0	149.09	0	431.8
3	90.0	0	90	-20.32
4	0.0	433.07	-90	0
5	0.0	0	90	0
FLANGE	0.0	56.25	0	0

IV. Simulation Studies

Simulation studies were conducted to assess the performance of proposed solution method. When measurement noise was not present, it was found that the procedure discussed in Section II produces exact results if singular points were removed (those points that correspond to $\theta_A \equiv \pi$).

To investigate the robustness of the procedures in the presence of measurement noise, the nominal PUMA robot geometry was chosen for simulation using the Denavit–Hartenberg (D–H) parameters listed in Table I.

Note that the listed values for θ_i in Table I are joint offsets at the arm home position.

Two arbitrarily chosen homogeneous transformations for simulating "actual" **BASE** and **TOOL** are given in (41).

$$\mathbf{BASE} = \begin{bmatrix} -0.99908 & -0.03266 & 0.02786 & 164.226 \\ 0.02737 & 0.01553 & 0.99950 & 301.638 \\ -0.03308 & 0.99935 & -0.01462 & -962.841 \\ 0.00000 & 0.00000 & 0.00000 & 1.00000 \end{bmatrix} \tag{41a}$$

$$\mathbf{TOOL} = \begin{bmatrix} -0.97651 & -0.09468 & -0.19356 & 9.190 \\ 0.06362 & -0.98493 & 0.16082 & 5.397 \\ -0.20587 & 0.14473 & 0.96782 & 62.628 \\ 0.00000 & 0.00000 & 0.00000 & 1.00000 \end{bmatrix} \tag{41b}$$

One of three uniformly distributed random noise processes (denoted by $U[a, b]$, listed in Table II) was added to the Z-Y-Z Euler angles and positions of the tool to model measurement noise. Other measurement uncertainties were ignored. Noise level 1 represents the noise of a moderately accurate measurement instrument while Noise level 3 simulates that of a relatively inaccurate device.

In all test results presented in this section, 30 pose measurements uniformly spaced in the PUMA workspace were employed for verification purposes. Orientation errors and position errors are defined in terms of the Euclidian norm of pose position and orientation deviations, respectively. Three types of tests were conducted to explore the following three issues.

A. Number of Pose Measurements Required for Calibration

In this type of tests, the nominal PUMA geometry listed in Table I and Noise level 1 listed in Table II were adopted. Figs. 2 and 3 depict position and orientation errors against the number of pose measurements. The position error is defined as the norm of the

TABLE II
NOISE INJECTED TO "POSE MEASUREMENTS"

	Orientation noise (deg)	Position noise (mm)
Noise level 1	U[-0.01, 0.01]	U[-0.1, 0.1]
Noise level 2	U[-0.05, 0.05]	U[-0.1, 0.1]
Noise level 3	U[-0.05, 0.05]	U[-0.5, 0.5]

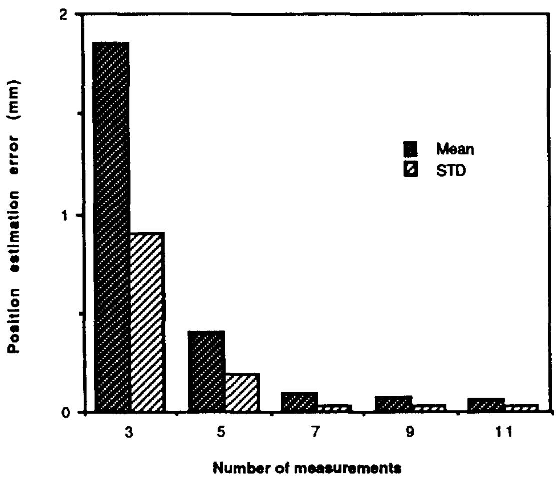

Fig. 2. Position errors against number of pose measurements.

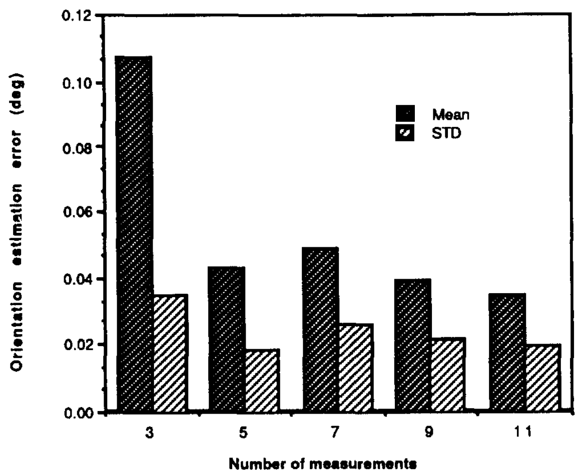

Fig. 3. Orientation errors against number of pose measurements.

difference between the computed position using the identified **BASE** and **TOOL** and the actual position obtained using the given **BASE** and **TOOL**. The orientation error is defined in a similar way.

It can be seen that pose errors were reduced when the number of pose measurements were increased, as seen from Fig. 2. This trend continues until adding more measurements would not significantly reduce pose errors. The threshold value for the number of pose measurements is around 6. Adding measurements can sometimes degrade the estimation quality, as seen in Fig. 3.

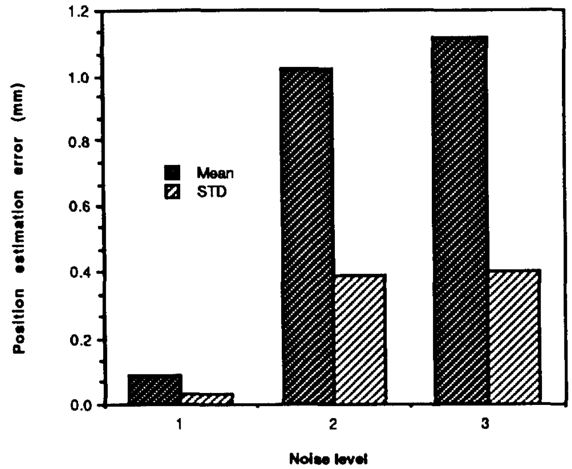

Fig. 4. Position errors against different levels of measurement noise.

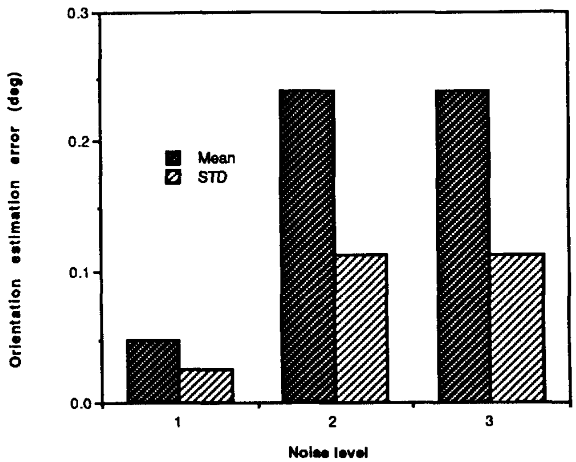

Fig. 5. Orientation errors against different levels of measurement noise.

B. Calibration Effectiveness Under Different Measurement Noise Levels

Figs. 4 and 5 show the pose errors under different noise levels with seven pose measurements being used. These figures suggest that pose errors using the identified **BASE** and **TOOL** transformations are roughly proportional to the intensity of the measurement noise. Furthermore, it was verified that pose orientation errors are independent of the accuracy of pose position measurements. However pose position errors depend on both orientation and position measurement accuracy.

C. Calibration Effectiveness When the Nominal Robot Geometry Deviates from Its Actual One and Joint Readings Are Not Perfect

To simulate an actual manipulator, uniformly distributed random noise processes were also injected to the PUMA joint variables and link parameters. Three noise models tested in the simulation are listed in Table III.

Model 1 represents a perfect robot and Model 3 is a fair representation of an actual one. The position and orientation errors exhibited by

TABLE III
NOISE INJECTED TO ROBOT LINK PARAMETERS AND JOINT VARIABLES

	Rotation parameters (deg)	Translation parameters (mm)	Joint variables (deg)
Model 1	U[0.0, 0.0]	U[0.0, 0.0]	U[0.0, 0.0]
Model 2	U[-0.01, 0.01]	U[-0.1, 0.1]	U[-0.01, 0.01]
Model 3	U[-0.05, 0.05]	U[-0.5, 0.5]	U[-0.05, 0.05]

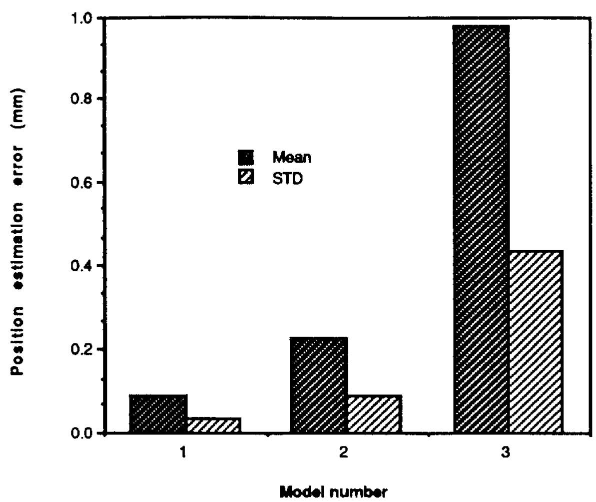

Fig. 6. Position errors against different levels of model uncertainties.

these models are listed in Figs. 6 and 7. The 1-mm figure for position errors contributed by Model 3 may be tolerable in some applications. If an application demands higher accuracy, users must consider a complete calibration of the robot. With complete calibration, PUMA arm's position errors can be reduced to within 0.4 mm [1].

V. CONCLUSION

A linear approach for robot simultaneous **BASE** and **TOOL** calibration by solving homogeneous transformation equations of the form $\mathbf{AX} = \mathbf{YB}$ has been presented in this paper. The method is applicable to most robots used in an off-line programming environment. When cameras are mounted on the robot hand, the eye-hand transformation can be treated as a special case of the tool-flange transformation, if the camera frame is considered as a "tool frame". The approach proposed in this paper can thus be applied to robot/world and eye/hand calibration. The results may also be useful to other problems that can be formulated into homogeneous transformation equations of the form $\mathbf{AX} = \mathbf{YB}$. Even though the derivations require the knowledge of quaternions algebra, the results do not. Users can easily implement the linear least squares procedure with minimal or no knowledge of advanced mathematical concepts.

A drawback of this approach is that since the geometric parameters of the system are estimated in a two-stage process, estimation errors from the first stage propagate to the second stage. Moreover, complete robot pose measurements are needed. While complete poses are not hard to obtain when hand-mounted cameras are used, this is considered to be a difficult and expensive task if other measurement

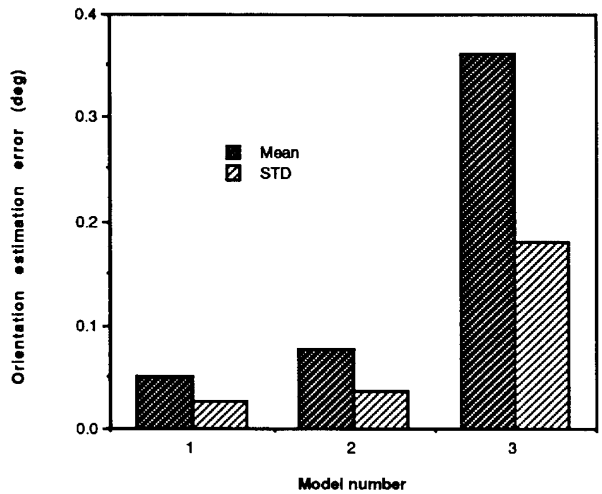

Fig. 7. Orientation errors against different levels of model uncertainties.

devices are employed. Some of the **BASE** and **TOOL** parameters become unobservable if one uses only partial pose information [9], [10].

REFERENCES

[1] B. Mooring, Z. S. Roth, and M. R. Driels, *Fundamentals of Manipulator Calibration.* New York: Wiley, 1991.
[2] Y. C. Shiu and S. Ahmad, "Calibration of wrist-mounted robotic sensors by solving homogeneous transform equations of the form $AX = XB$," *IEEE Trans. Robotics Automat.*, vol. 5, pp. 16–27, 1989.
[3] H. Zhuang and Z. S. Roth, "Comments on 'Calibration of wrist-mounted robotic sensors by solving homogeneous transformation equations of the form $AX = XB$'" *IEEE Trans. Robotics Automat.*, vol. 7, pp. 877–878, 1991.
[4] K. N. S. Rao, *The Rotation and Lorentz Groups and Their Representations for Physicists.* New York: Wiley, 1988, pp. 11–12, 146–152.
[5] J. C. K. Chou, "Quaternion kinematic and dynamic differential equations," *IEEE Trans. Robotics Automat.*, vol. 8, pp. 53–64, 1992.
[6] R. P. Paul, *Robot Manipulators: Mathematics, Programming and Control.* Cambridge, MA: MIT Press, 1981.
[7] *MACSYMA, Vax Unix Reference Manual*, ver. 11. Symbolics, Inc., 1985.
[8] R. Y. Tsai and R. K. Lenz, "A new technique for fully autonomous and efficient 3-d robotics hand/eye calibration," *IEEE Trans. Robotics Autom.*, vol. 5, pp. 345–357, June 1989.
[9] L. J. Everett and T. W. Hsu, "The theory of kinematic parameter identification for industrial robots," *ASME J. Dynamic Syst., Measurements, and Control*, vol. 110, no. 1, pp. 96–100, 1988 .
[10] H. Zhuang, Z. S. Roth, and F. Hamano, "Observability issues in kinematic error parameter identification of manipulators," *ASME J. Dynamic Syst., Measurements, and Control*, vol. 114, no. 2, pp. 319–322, 1992.